Western Diet Promotes Intestinal Colonization by Collagenolytic Microbes and Promotes Tumor Formation After Colorectal Surgery

Gaines, Sara; van Praagh, Jasper B; Williamson, Ashley J; Jacobson, Richard A; Hyoju, Sanjiv; Zaborin, Alexander; Mao, Jun; Koo, Hyun Y; Alpert, Lindsay; Bissonnette, Marc

Published in:
Gastroenterology

DOI:
10.1053/j.gastro.2019.10.020

Publication date:
2020

Gastroenterology 2020;158:958–970

Western Diet Promotes Intestinal Colonization by Collagenolytic Microbes and Promotes Tumor Formation After Colorectal Surgery

Sara Gaines,[1] Jasper B. van Praagh,[1,2] Ashley J. Williamson,[1] Richard A. Jacobson,[1,3] Sanjiv Hyoju,[1] Alexander Zaborin,[1] Jun Mao,[1] Hyun Y. Koo,[1] Lindsay Alpert,[1] Marc Bissonnette,[1] Ralph Weichselbaum,[1] Jack Gilbert,[1,4] Eugene Chang,[1] Neil Hyman,[1] Olga Zaborina,[1,§] Benjamin D. Shogan,[1,§] and John C. Alverdy[1,§]

[1]University of Chicago, Pritzker School of Medicine, Chicago, Illinois; [2]University of Groningen, University Medical Center Groningen, Groningen, The Netherlands; [3]Rush University Medical Center, Chicago, IL; and [4]University of California–San Diego, Department of Pediatrics, La Jolla, California

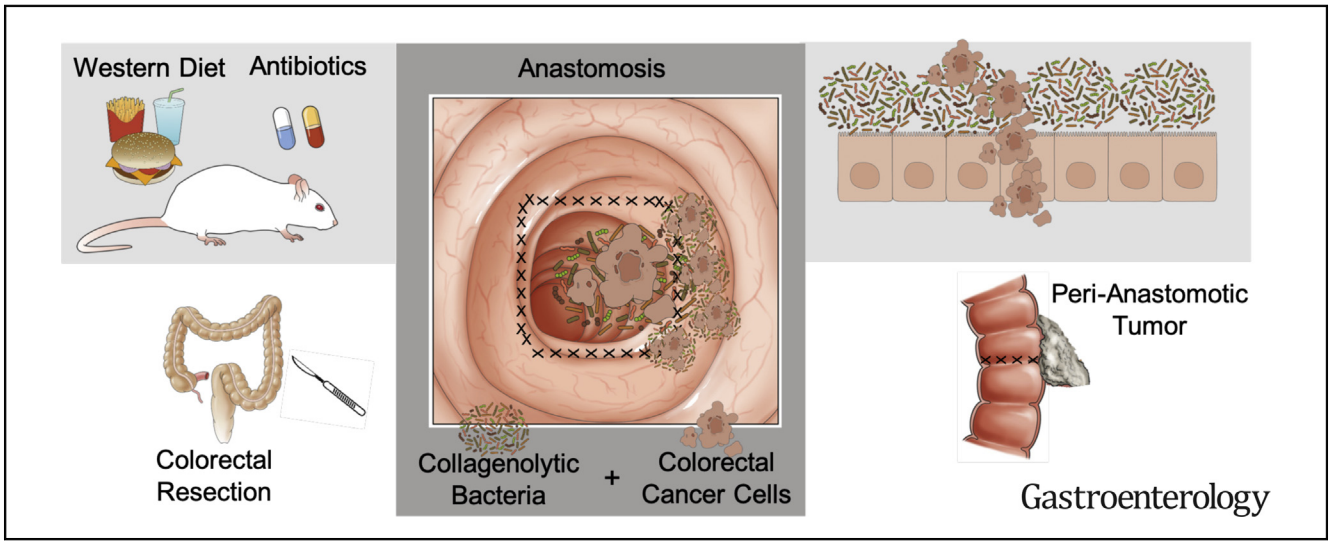

See Covering the Cover synopsis on page 796.

BACKGROUND & AIMS: The Western diet, which is high in fat, is a modifiable risk factor for colorectal recurrence after curative resection. We investigated the mechanisms by which the Western diet promotes tumor recurrence, including changes in the microbiome, in mice that underwent colorectal resection. **METHODS:** BALB/c male mice were fed either standard chow diet or Western-type diet (characterized by high fat, no fiber, and decreased minerals and vitamins) for 4 weeks; some mice were given antibiotics or ABA-PEG20k-Pi20 (Pi-PEG), which inhibits collagenase production by bacteria, but not bacterial growth, in drinking water. Colorectal resections and anastomoses were then performed. The first day after surgery, mice were given enemas containing a collagenolytic rodent-derived strain of *Enterococcus faecalis* (strain E2), and on the second day they were given mouse colon carcinoma cells (CT26). Twenty-one days later, distal colons were removed, and colon contents (feces, distal colon, and tumor) were collected. Colon tissues were analyzed by histology for the presence of collagenolytic colonies and by 16S ribosomal RNA sequencing, which determined the anatomic distribution of *E faecalis* at the site of the anastomosis and within tumors using in situ hybridization. Mouse imaging analyses were used to identify metastases. **RESULTS:** Colorectal tumors were found in 88% of mice fed the Western diet and given antibiotics, surgery, and *E faecalis* compared with only 30% of mice fed the standard diet followed by the same procedures. Colon tumor formation correlated with the presence of collagenolytic *E faecalis* and *Proteus mirabilis*. Antibiotics eliminated collagenolytic *E faecalis* and *P mirabilis* but did not reduce tumor formation. However, antibiotics promoted emergence of *Candida parapsilosis*, a collagenase-producing microorganism. Administration of a Pi-PEG reduced tumor formation and maintained diversity of the colon microbiome. **CONCLUSIONS:** We identified a mechanisms by which diet and antibiotic use can promote tumorigenesis by colon cancer cells at the anastomosis after colorectal surgery. Strategies to prevent emergence of these microbe communities or their enzymatic activities might be used to reduce the risk of tumor recurrence in patients undergoing colorectal cancer surgery.

Keywords: CRC; Progression; Carcinogenesis; Prevention of Recurrence.

WHAT YOU NEED TO KNOW

BACKGROUND AND CONTEXT

The western diet, which is high in fat, is a risk factor for colorectal recurrence after curative resection. We investigated the mechanisms by which a western diet promotes tumor recurrence, including changes in the microbiome, in mice that underwent colorectal resections.

NEW FINDINGS

We identified mechanisms by which colon cancer cells at the anastomosis following colorectal surgery can reform tumors, and how factors such as diet and antibiotic use, which promote emergence of collagenolytic bacteria, contribute to recurrence.

LIMITATIONS

This study was performed in mice; further studies are needed in patients.

IMPACT

Strategies to prevent emergence of these microbe communities or their enzymatic activities might be used to prevent tumor recurrence in patients undergoing colorectal cancer surgery.

Nearly 140,000 new cases of colorectal cancer (CRC) are diagnosed annually and, despite advances in its treatment, CRC remains a leading cause of death.[1] The lethal nature of CRC is attributed to a 15% rate of local and 25% rate of distal recurrence after surgical resection.[2] Although local recurrence is presumed to be a function of microscopic tumor left behind during the index operation, emerging evidence suggests a more central role for the biology of the primary tumor itself.[3] Unique to gastrointestinal malignancies is the inevitable presence of shed cancer cells in the lumen of the colon exfoliated from the primary tumor during growth or surgical manipulation.[4–6] Although the surgical reconnection of the intestine after resection (termed *anastomosis*) is intended to be impermeable, animal studies have determined that shed cancer cells can penetrate the anastomosis, resulting in local recurrence.[7,8] However, the selective pressures in the local anastomotic environment that promote shed cancer cells to penetrate an intact anastomosis and form tumors are incompletely understood.

Previous work from our laboratory has shown that the anastomotic environment can act as a chemoattractant for collagenase-producing intestinal microbiota (ie, *Enterococcus faecalis*) that can disrupt a surgically intact anastomosis.[9,10] Prior antibiotics, preoperative chemoradiation, and diet may further promote these pathobionts to predominate on anastomotic tissues, causing tissue breakdown and clinical leakage.[11,12] Because anastomotic leaks are strongly associated with local CRC recurrence, it is possible that local conditions at the site of a disrupted anastomosis may create opportunities for shed cancer cells to penetrate tissue and form tumors.[13–15]

Multiple aspects of the pathogenesis of CRC are now known to be influenced by the intestinal microbiome.[16–18] It has emerged that diet has a profound effect on both the composition and function of the microbiome.[19] The finding that patients consuming a high-fat, Western-type diet after colorectal cancer resection have higher rates of recurrence suggests a link between diet, its influence on the microbiome, and microbiome-mediated changes in intestinal epithelial function.[20,21] This is not surprising given that the intestinal microbes mediate the interface between our environment and our genes and provide a proposed mechanism by which various disorders such as colon cancer, diabetes, obesity, and autoimmune disease develop.[22,23]

In this study, we sought to combine the various elements that occur in the setting of colon cancer surgery that might predispose to locoregional tumor formation, such as a high-fat/low-fiber Western diet (WD), exposure to prophylactic antibiotics, colonization with strains of collagenolytic *E faecalis*, and exposure of anastomotic tissues to shed colon cancer cells. We hypothesized that diet-induced alterations in the intestinal microbiota promote anastomotic penetration of shed cancer cells, resulting in tumor formation. Therefore, the aim of the study was to show that alterations in the intestinal microbiota that develop from the combined exposure to a WD, antibiotics, and collagenolytic *E faecalis* can render anastomotic tissues susceptible to local tumor formation after luminal exposure to a murine colon cancer cell line. Results indicate that a technically adequate colorectal anastomosis can be rendered permeable to dispersed colon cancer cells when a WD and antibiotics promote the colonization of collagenolytic pathobiota on anastomotic tissue.

BASIC AND TRANSLATIONAL AT

Materials and Methods

Mouse Model of Colorectal Anastomosis

BALB/c male mice aged 8–10 weeks (Charles River Laboratories, Wilmington, MA) were used and maintained according to Institutional Animal Care and Use Committee 72491. We used a previously validated mouse model of a colon resection and anastomosis.[10] Mice were fed either standard chow diet (std) or WD (BioServeS3282; Hunterdon County, NJ), characterized by high fat, no fiber, and decreased minerals and vitamins compared with std (Supplementary Table 1), for 4 weeks before the day of surgery. One hour before surgery, all animals received 40 mg/kg intramuscular cefoxitin (Henry Schein, Melville, NY) and 100 mg/kg oral clindamycin (Henry Schein) and then underwent general anesthesia with 100 mg/kg

§ Authors share co-senior authorship.

Abbreviations used in this paper: bp, base pair; CFU, colony-forming unit; CRC, colorectal cancer; MBP, mechanical bowel preparation; PCR, polymerase chain reaction; Pi-PEG, ABA-PEG20k-Pi20; POD, postoperative day; RFU, relative fluorescence unit; std, standard chow diet; WD, Western diet.

Most current article

0016-5085/$36.00
https://doi.org/10.1053/j.gastro.2019.10.020

intraperitoneal ketamine (Henry Schein) and 10mg/kg xylazine (Henry Schein). In select experiments, animals were administered a rectal enema with 100 μL of solution on postoperative day (POD) 1 or 2 using a 22-gauge blunt-tip needle.

Anesthetic complications occurred in <10% of animals, and animals were added to achieve equal numbers. The remaining animals appeared normal after surgery and until they were killed on POD 21. Mice fed a WD were of the same weight as mice fed a std diet, consistent with studies showing the resistance of BALB/c mice to weight gain induced by a high-fat diet.[24]

Bacterial Strain and Preparation for Administration

The *E faecalis* E2 strain used in this study was previously isolated from anastomotic rat tissue.[9] The E2 strain, recovered directly from stock frozen at –80°C in 10% glycerol, was grown on selective enterococcal agar (BBL Enterococcosel agar; BD Diagnostics, Franklin Lakes, NJ) for 24 hours before inoculation. On POD 1, an E2 suspension was made with an optical density of 0.5 (600 nm) in sterile 10% glycerol (1×10^8 colony-forming units [CFU]/mL).

Murine Colorectal Cancer Strain and Preparation for Administration

Luciferase/tdTomato-labeled monoclonal (L2T) CT26 cells, a modification of CT26.WT (ATCC CRL-2638) colon carcinoma cell line derived from BALB/c mice, created by Ralph Weichselbaum, were used.[25] To create the aliquots used for injection, 1×10^6 L2T CT26 (hereafter termed *CT26*) was thawed and grown in Dulbecco's modified Eagle medium supplemented with 10% fetal bovine serum, 100 U/mL penicillin, and 100 mg/mL streptomycin and maintained in culture at 5% CO_2 and 37°C. At 80% confluency, cells were removed, washed, and resuspended in Hank's balanced salt solution. A total of 1×10^5 cells in 100 μL were injected via enema (described earlier).

Animal Tissue Analysis and Collection

Animals were killed on POD 21, and each abdomen was opened. The peritoneum and liver were inspected for grossly visible metastases. The distal colon was resected from the splenic flexure to the rectal margin to encompass the anastomosis and extraluminal tumor. The colon was opened longitudinally, and the luminal contents were removed. A portion of the feces, distal colon, and tumor (if present) were each placed in 500 μL of sterile saline for DNA isolation and in sterile 10% glycerol for microbial culture. In a subset of animals, the distal colon and tumor were submitted for histologic analysis (discussed in the following sections). The determination of tumor was made by visual inspection and confirmed by histology (discussed in the following sections) in selected samples. After initial histologic confirmation, the determination of subsequent tumor formation was made by visual inspection. For micrometastatic analysis via reverse-transcription polymerase chain reaction (PCR), the liver was removed in its entirety and placed in 1.5 mL sterile saline.

Histology and Trichrome Staining

Distal colon and tumor were fixed in 10% formalin and washed in 70% ethanol. H&E staining was performed on embedded tissue cut into 5-μm slices. Trichrome staining was used to detect collagen.

Microbial Culture for Collagenase Activity

Homogenized colon tissue and luminal content aliquots were thawed and serially diluted. Then, 20 μL of each dilution was plated onto skim milk–containing Enterococcosel agar (15% skim milk; US Biological Life Sciences, Swampscott, MA), and MacConkey agar (Difco, Franklin Lakes, NJ) (20% skim milk), prepared as previously described.[26] Collagenolytic colonies were identified at the University of Chicago Clinical Microbiology Laboratory. The CFU count was normalized to sample weight.

DNA Isolation

Each sample was homogenized with the FastPrep-24 5G Instrument (MP Biomedicals, Santa Ana, CA). Total DNA was extracted from 300 μL of homogenate with the FastDNA SPIN KIT (MP Biomedicals).

16S Ribosomal RNA Gene Analysis

Total DNA obtained from the mouse samples was used as template DNA. Each 25-μL PCR reaction contained 12.5 μL AccuStart II PCR ToughMix (Quantabio, Beverly, MA), 8.5 μL of PCR-grade water, 1 μL forward primer, 1 μL mPNA (50 μmol/L) (PNA Bio, Thousand Oaks, CA) to block host target mitochondrial contamination, 1 μL Golay Barcode Tagged Reverse Primer (5 μmol/L), and 1 μL template DNA. The PCR conditions were 94°C for 3 minutes followed by 35 cycles at 94°C for 45 seconds, 50°C for 60 seconds, and 72°C for 90 seconds, with a final extension of 10 minutes at 72°C. The amplicons were cleaned, pooled, and quantified using the Quant-iT PicoGreen (Invitrogen, Carlsbad, CA) double-stranded DNA assay kit following EMP (Earth Microbiome Project) benchmarked protocols.[27] Pooled amplicons were then pair-end sequenced (2 × 150 base pairs [bp]) on an Illumina (San Diego, CA) MiSeq sequencing run at the Argonne National Laboratory.

Bacterial 16S V4 region (515F–806R primer pair) sequences were processed with Qiime2 (v2018.6).[28,29] Default parameters were used for demultiplexing. Quality control was performed with the DADA2 function integrated in Qiime2 to truncate forward and reverse reads, to denoise the data, and for detection and removal of chimeras.[30] The representative sequence variants of each sample were retained and assigned to bacterial taxa using a naive Bayes classifier trained on the Greengenes 13_8 99% operational taxonomic units.[31]

Statistical analyses were performed in R, version 3.5.1 (R Core Team, Vienna, Austria) and Qiime2 on rarefied data (depth of 2850 reads). Differential abundance and taxa dissimilarities across study groups were analyzed using the Kruskal-Wallis analysis of variance (ANOVA) test with the R package DESeq2. All P values were corrected for multiple comparisons by the Benjamini-Hochberg false discovery rate procedure and were considered significant at an adjusted P value (P_{adj}) < .05.

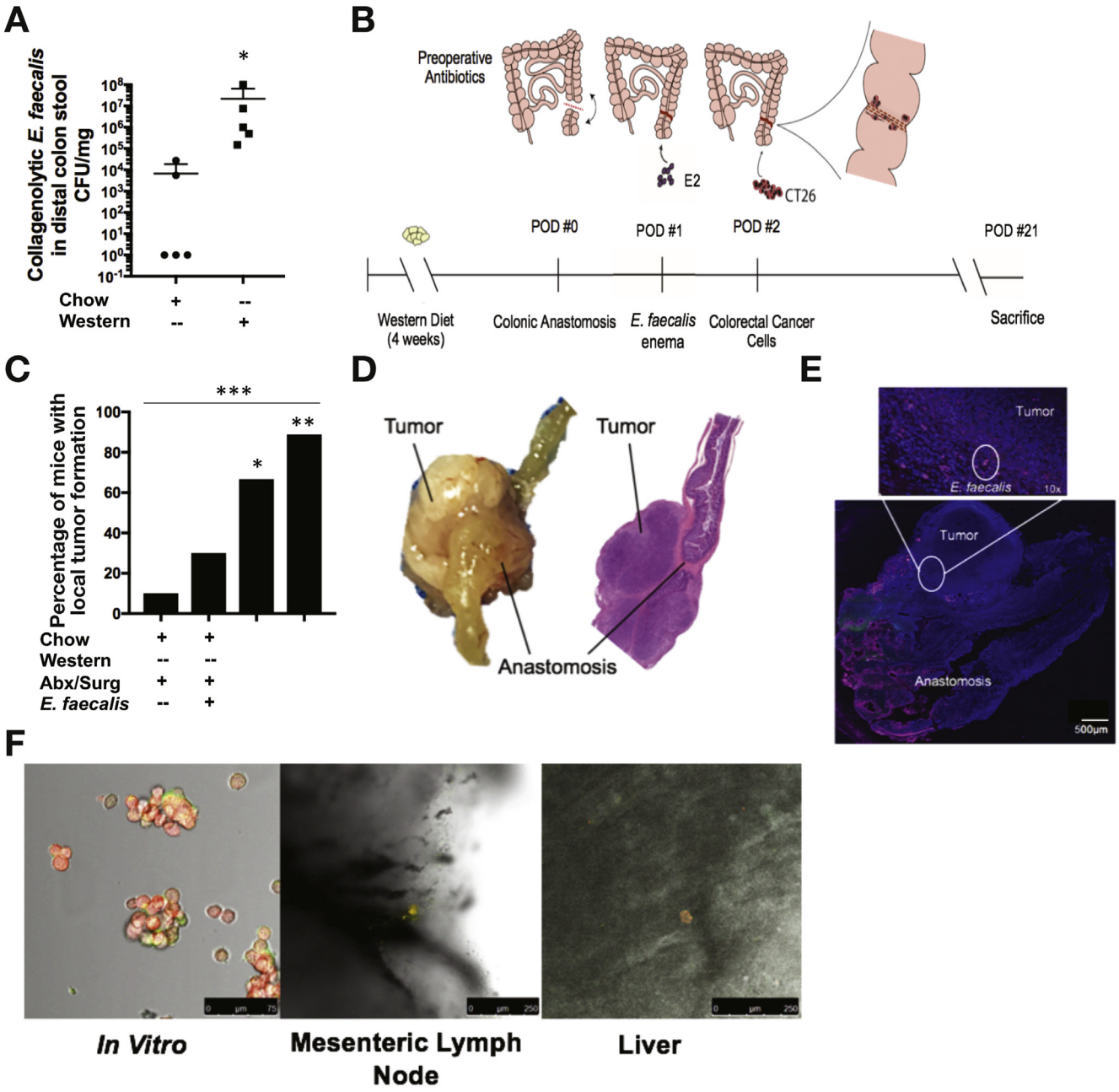

Figure 1. Model of colorectal tumor formation in mice after surgery. (*A*) Mice fed a WD resulted in an increase of nearly 3-orders of magnitude (6.6×10^3 vs 2.18×10^7 CFU/mg; n = 5 per group; $P < .05$, Mann-Whitney test) in collagenolytic *E faecalis* in the distal colon. (*B*) Mouse model of anastomotic colon tumor formation: mice are fed a WD or std diet for 4 weeks, after which they are administered oral clindamycin and parenteral cefoxitin before surgery and then subjected to colorectal anastomosis. On POD 1, anastomotic tissues are exposed to collagenolytic *E faecalis* via enema. On POD 2, anastomotic tissues are exposed to CRC cells (CT26) via enema. All animals are killed on POD 21. (*C*) A perianastomotic, extramucosal tumor formation was seen in 67% (n = 8/12) of mice fed the WD compared with 10% of animals fed the std diet (n = 1/10; $P <$ .05, Fisher exact test). Exposure of anastomotic tissues to *E faecalis* increased tumor formation to 88% in WD-fed mice compared with 30% in std-fed mice ($n \geq 10$ per group; $P < .05$, Fisher exact test). Differences in tumor formation among the groups was statistically significant. There were also significant differences in tumor incidence between control std diet–fed mice and WD-fed mice given *E faecalis* ($P < .05$, ordinary 1-way ANOVA). (*D*) Representative gross tumors (*left*) and H&E staining histology (*right*) showed extramucosal tumor formation. (*E*) Fluorescence in situ hybridization for *E faecalis* (*pink*) showed *E faecalis* colonization in anastomotic tissue and throughout the colonic tumor. (*F*) Representative confocal imaging showing tomato-labeled CT26 cells in mesenteric lymph nodes and liver tissue in a WD-fed mouse administered an *E faecalis* enema. Abx, antibiotics; Surg, surgery. *significance of $p<.05$

Fluorescence In Situ Hybridization

To visualize *E faecalis* on paraffin-embedded tissue, we used fluorescence in situ hybridization beacon-based technology. The probe was labeled with *E faecalis*–specific Alexa Fluor 647 (Miacom Diagnostics; Dusseldorf, Germany). We used confocal microcopy on a Leica (Wetzlar, Germany) SP5II AOBS tandem scanner spectral confocal system on a DMI6000 microscope. The Leica microscope is controlled by LASAF software, version 2.8.3, with an excitation/emission of 654/d755 nm. Objectives used were ×20, NA0.7 dry; ×10, NA0.4 dry; and ×40, NA1.25 oil.

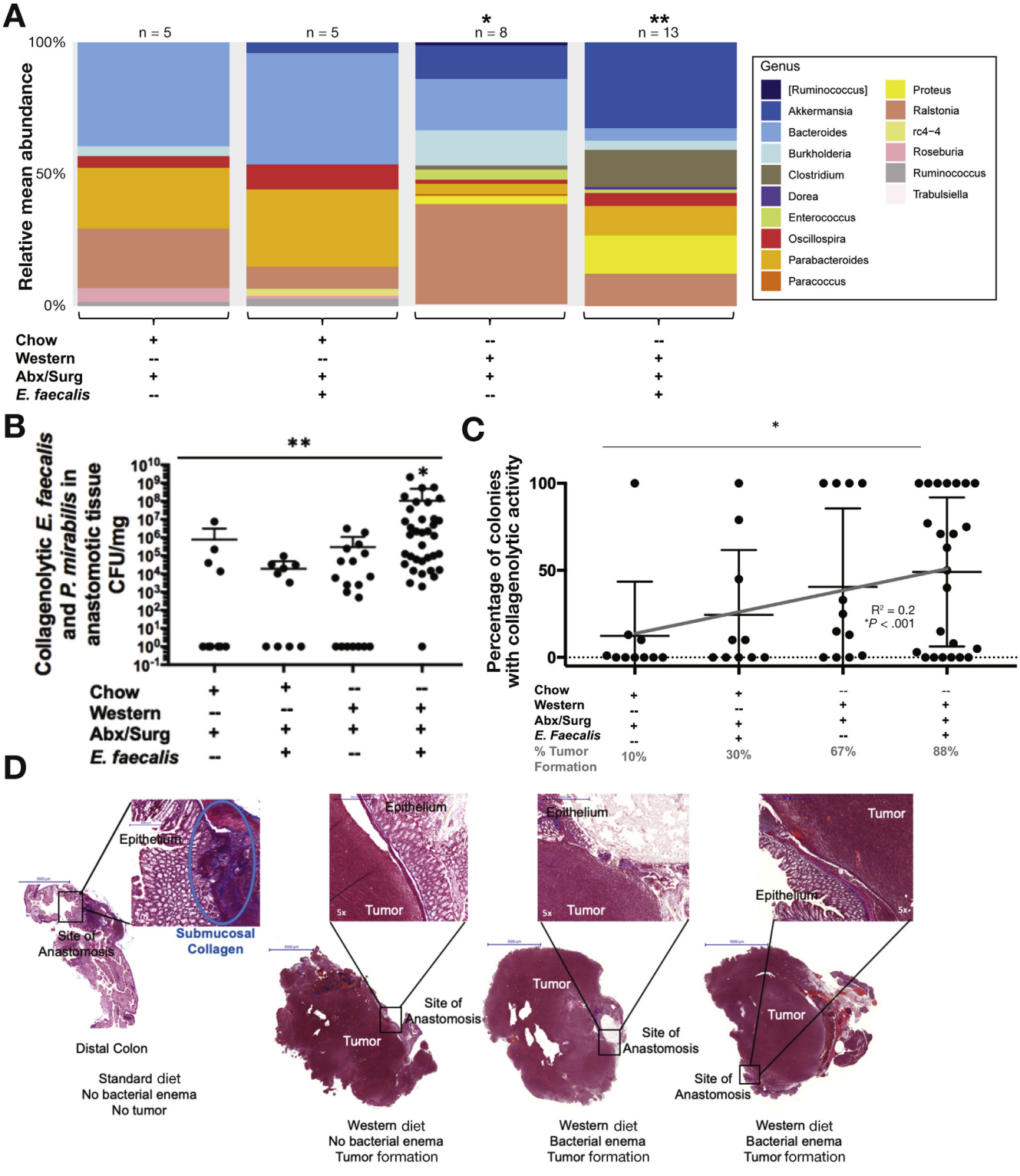

Additional Experimental Antibiotics

Vancomycin 4 mg/kg (Med Vet International, Mettawa, IL), ampicillin 50 g/kg (Med Vet International), spectinomycin 500 μg/mL (Henry Schein Animal Health), and streptomycin 15 μg/mL (Henry Schein Animal Health) were dissolved in 500 mL drinking water.

ABA-PEG20k-Pi20

The polyphosphate-containing polyethylene glycol–based triblock copolymer was synthesized as previously described.[32] ABA-PEG20k-Pi20 (Pi-PEG) was adjusted to pH 7.4 and added to a 1% final solution to the drinking water of animals in select experiments. The pH was adjusted weekly to maintain pH 7.4.

Collagenase Assay of Selected Strains

The collagenase activity of selected strains was measured by using fluorescein-labeled gelatin or fluorescein-labeled collagen (EnzChek Gelatinase/Collagenase assay kit; Thermo Fisher Scientific, Waltham, MA). Samples were suspended in TY medium with 10 g/L tryptone and 5 g/L yeast extract, as previously described.[9] In select experiments, Pi-PEG was added to a final concentration of 1%. Fluorescence (485/20 nm excitation, 528/20 nm emission) and OD 600 nm were measured at 0, 4, 12, and 24 hours. Zero-hour values were subtracted from time points, and samples were normalized for bacterial growth. To assess collagenase activity in *Candida* species, the assay was performed identically but continued for an additional 48 hours because the peak change in optical density occurs between 24 and 48 hours for this organism.

Metastatic Imaging

Freshly harvested tissues on POD 21 were placed in a Petri dish with 20 μL saline and immediately analyzed with the Leica SP5II AOBS tandem scanner spectral confocal system on a DMI6000 microscope for tomato fluorescence with excitation/emission of 400/600 nm.

Quantitative Polymerase Chain Reaction

For quantitative analysis of CT26 cells in the liver, quantitative PCR was used (QuantStudio 3 System; Thermo Fisher Scientific). A TaqMan primer-probe was designed to identify the luciferase (luc2) gene (Supplementary Table 2) (Primetime Gene Expression Master Mix; Integrated DNA Technologies, Coralville, IA). All threshold cycle values of the *luc2* gene were analyzed by Quantstudio Design and Analysis Software (Thermo Fisher Scientific) with an automatically generated threshold.

Stool Biobanking Study

Stool samples from patients ≥18 years undergoing an elective colon resection at the University of Chicago were collected between September 2017 and September 2018 (institutional review board 17-0417). Preoperative stool samples obtained before bowel preparation were collected using the BioCollector stool kit (BioCollective, Denver, CO). Intraoperative samples were collected by rectal examination after the induction of general anesthesia.

Statistical Analysis

Statistical analyses were performed with GraphPad Prism 8 (GraphPad Software, San Diego, CA). Paired Student *t* tests was used for comparisons between 2 means. The Mann-Whitney nonparametric test was used when there was no assumption of normal distribution. The Fisher exact test was used to describe 2 categorical values. Ordinary 1-way ANOVA was used to compare the means of 2 or more samples. Kruskal-Wallis 1-way ANOVA was used to compare ≥2 independent samples of equal or different samples sizes. The 16S ribosomal RNA analyses were described earlier. Statistical significance was defined as $P < .05$. A mixed-effects model was used to allow for correlation between repeated measurements on a subset of individuals in the stool biobanking study. This model included main effect terms for weight group and timing of bowel preparation, as well as a group-by-time interaction. A statistically significant interaction indicated that the magnitude of the before and after bowel preparation changes differed between normal and obese mice.

Results

Mice Fed a Western Diet Form Extraintestinal Tumors After Luminal Exposure to Collagenase-Producing Enterococcus faecalis and Shed Colon Cancer Cells

To determine the influence of a high-fat/no-fiber WD on the intestinal microbiota, BALB/c male mice were placed on 4 weeks of a polyunsaturated fatty acid diet consisting of 60% fat calories and no fiber vs std consisting of 6.2% fat and 3.5% crude fiber (Supplementary Table 1). Compared with std, WD-fed mice showed a rate of colonization that was 3 orders of magnitude higher with collagenolytic *E faecalis* in the distal colon (2.9×10^7 vs 6.6×10^3 CFU/mg; $P < .05$, Mann-Whitney test) (Figure 1*A*). Next, groups of mice were assigned to 4 weeks of feeding of either WD or std. Because patients undergoing colon surgery receive both oral and parenteral prophylactic antibiotics, animals were

Figure 2. Tumor formation is associated with collagenolytic *E faecalis* and *P mirabilis* in anastomotic Tissues. (*A*) The 16S ribosomal RNA taxonomic proportions showed that mice fed a WD harbor a significant increase in the proportion of *Proteus* species and a significant increase in both *Proteus* and *Enterococcus* when administered *E faecalis* compared with std-fed mice ($P_{adj} < .05$). (*B*) Colonization of anastomotic tissues with collagenolytic *E faecalis* or *P mirabilis* was increased in WD-fed mice after *E faecalis* enema (8.8×10^7 vs 2.9×10^5 CFU/mg, n ≥ 10 per group; $P < .05$, Mann-Whitney test). Colonization of collagenolytic *E faecalis* and *P mirabilis* was statistically significant among all groups ($P < .05$, Kruskal-Wallis test). (*C*) Analysis of the percentage of bacterial colonies with collagenase activity compared with total bacteria showed a linear correlation between incidence of local tumor formation and collagenolytic burden in the anastomotic tissues (n ≥ 10 per group; $P < .05$; ordinary 1-way ANOVA, $R^2 = 0.2$). (*D*) Trichrome collagen stain showed a decrease in submucosal collagen fibers (*blue*) in tumor-forming mice, with minimal collagen present between the tumor and adjacent mucosa. Abx, antibiotics; Surg, surgery.

administered oral clindamycin and intramuscular cefoxitin and then subjected to colorectal resection and subsequent anastomosis. To ensure equal exposure of anastomotic tissues to collagenolytic *E faecalis* in both std- and WD-fed mice, a previously characterized collagenolytic rodent-derived strain of *E faecalis* (strain E2) was delivered via enema on POD 1 (Figure 1*B*). Finally, to mimic the exposure of anastomotic tissues to shed cancer cells, an inevitable occurrence both during and after surgery, dispersed mouse colon cancer cells (CT26) were administered by enema on POD 2.

Based on preliminary data showing that tumors required approximately 21 days to form in this model, mice were killed on POD 21. Necropsy found the presence of peri-anastomotic, extramucosal tumor formation in 67% (8/12) of WD-fed mice compared with 10% (1/10) of std-fed mice ($P < .05$, Fisher exact test). Exposure of anastomotic tissues to collagenolytic strains of *E faecalis* via enema resulted in a significant increase in tumor formation (88% in WD-fed mice vs 30% in std-fed mice; $P < .05$, Fisher exact test). The percentage of mice with local tumor formation across all groups was statistically significant ($P < .05$, ordinary 1-way ANOVA) (Figure 1*C* and *D*). Finally, when mice were killed, the colon was opened, and no mucosal tumors were observed; instead, a well healed anastomosis was identified, as judged by our validated healing score of 1 (loose adhesion) or 2 (dense adhesion) in all groups of mice.[33]

We next determined the anatomic distribution of *E faecalis* at the site of the anastomosis and within tumors using fluorescence in situ hybridization. We found that *E faecalis* co-aggregated in peri-anastomotic tissues and were scattered throughout the tumor (Figure 1*E*).

To determine if intraluminally introduced CT26 cells penetrated beyond the anastomotic tumor site, we used imaging to detect the presence of the dual-labeled CT26 cells (luciferase and tomato) with the Leica sp2_photon tandem scanner. Analysis of the images showed micrometastases in mesenteric lymph nodes and in the liver of WD-fed mice inoculated with *E faecalis* via enema (Figure 1*F*). Reverse-transcription PCR of the *luc2* gene of the CT26 cells in livers of mice fed a WD vs a std diet found that animals fed a WD had a trend toward an increase in the incidence of liver micrometastases compared with std-fed animals (40% vs 10%; $P = .1$, Fisher exact test) (Supplementary Figure 1).

Anastomotic Enterococcus faecalis *or* Proteus mirabilis *Colonization Significantly Correlates With Tumor Formation*

The compositional changes of the anastomotic microbiome that are associated with tumor formation were determined using 16S ribosomal RNA sequencing, which indicated that WD-fed mice (n = 8) had a significant increase in the proportion of the bacterial genera *Proteus* ($P_{adj} = .005$), *Akkermansia* ($P_{adj} = .001$), and *Trabulsiella* ($P_{adj} = 1.81 \times 10^{-11}$) but a decrease in *Bacteroides* ($P_{adj} = .027$), *Roseburia* ($P_{adj} = 5.82 \times 10^{-15}$), and *Ruminococcus* ($P_{adj} = .048$) compared with std diet–fed mice (n = 5). The relative mean abundance in the subset of animals in which *E faecalis* was introduced showed a bloom in the genera *Proteus* ($P_{adj} = 9.52 \times 10^{-14}$), *Enterococcus* ($P_{adj} = 9.52 \times 10^{-14}$), *Trabulsiella* ($P_{adj} = .008$), *Akkermansia* ($P_{adj} = .033$), and *Clostridium* ($P_{adj} = .012$), whereas the genus *Roseburia* proportionally decreased ($P_{adj} = 2.98 \times 10^{-5}$) in WD-fed mice (n = 13) (Figure 2*A*). Results regarding the absolute quantity (pg/μL) of the *Enterococcus* and *Proteus* genera displayed a similar pattern (Supplementary Table 3).

Our previous work showed that both *P mirabilis* and *E faecalis* express a collagenolytic phenotype capable of disrupting the integrity of anastomotic tissues. Given the observation that both *Proteus* and *Enterococcus* species were increased in WD-fed mice (which displayed the highest incidence of tumor formation), we next examined the bacterial collagenase activity of *E faecalis* or *P mirabilis* across all of the groups. There was a significant difference in the colonization density of collagenolytic *E faecalis* and *P mirabilis* between all groups ($P < .05$, Kruskal-Wallis test) (Figure 2*B*). An increase of approximately 3 orders of magnitude in the density of collagenolytic bacteria was observed between WD-fed mice compared with std-fed mice (8.8×10^7 vs 2.9×10^5 CFU/mg; $P < .05$, Mann-Whitney test) when exposed to the elements of the model (*E faecalis* enema, antibiotics, surgery). Further analysis of the percentage of total bacterial colonies with collagenolytic activity compared with the total bacteria present in the anastomotic tissue showed a linear correlation between the percentage of tumor formation and collagenase activity when collagenolytic *E faecalis* and *P mirabilis* activities were combined ($P < .05$; ordinary 1-way ANOVA, $R^2 = 0.2$) (Figure 2*C*). Trichrome staining for collagen showed a reduction in submucosal collagen in mice with local tumor formation, consistent with increased collagenase activity (Figure 2*D*).

Antibiotics Directed at Eliminating Collagenolytic Pathobiota Failed to Reduce Tumor Formation but Selected for the Emergence of Fungal Collagenase-Producing Microorganisms

To validate its role in tumor formation, *E faecalis* eradication was attempted in WD-fed mice by using oral vancomycin treatment on the day before surgery and continued throughout the study period. To our surprise, there was no difference in tumor formation (50% vs 40%; $P = .17$, Fisher exact test) or tumor-associated collagenolytic microbes (2.9×10^5 vs 1.8×10^6 CFU/mg; $P = .2$, Mann-Whitney test) between animals receiving vancomycin and controls (Figure 3*A*). However, vancomycin treatment resulted in a significant disruption of the bacterial community, characterized by the reduced relative abundance of all phyla that predominated (Firmicutes [$P_{adj} = 1.11 \times 10^{-7}$], Verrucomicrobia [$P_{adj} = 1.51 \times 10^{-4}$], and Bacteroidetes [$P_{adj} = 5.18 \times 10^{-4}$]), except for an increase of Proteobacteria ($P_{adj} = 1.11 \times 10^{-7}$) (Figure 3*B*). Compared with the non–vancomycin-treated controls, a proportional decrease in *Bacteroides* ($P_{adj} = 1.07 \times 10^{-20}$), *Clostridium* ($P_{adj} = 2.31 \times 10^{-4}$), *Dorea* ($P_{adj} = 3.09 \times 10^{-9}$), *Akkermansia* ($P_{adj} = 8.00 \times 10^{-7}$), and *Parabacteroides* ($P_{adj} = 5.18 \times 10^{-5}$) was

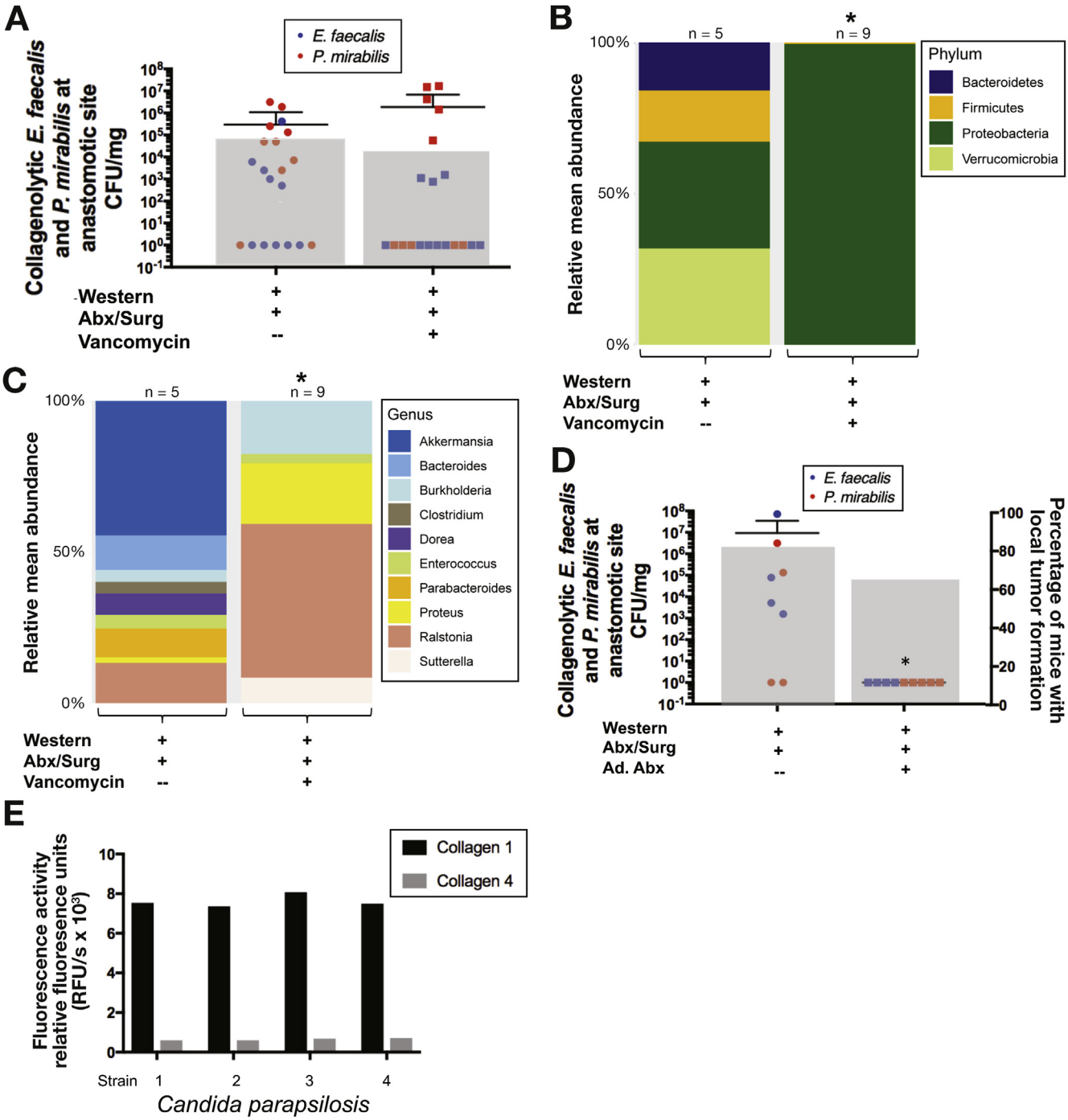

Figure 3. Broadening the antibiotic coverage in the model resulted in the emergence of additional collagenase-producing fungal organisms but did not prevent tumor formation. (*A*) To eradicate *E faecalis* and validate its role in tumor formation, animals were given vancomycin starting the day before surgery and continuing until they were killed. Vancomycin failed to reduce both the total tumor-associated collagenolytic microbes (2.9×10^5 vs 1.8×10^6 CFU/mg; n = 10 per group; $P = .2$, Mann-Whitney test) and tumor formation (50% vs 40%; n = 10 per group; $P = .17$, Fisher exact test). (*B*) Treatment with vancomycin significantly disrupted organization on the phylum level by diminution of Firmicutes ($P_{adj} = 1.11 \times 10^{-7}$), Verrucomicrobia ($P_{adj} = 1.51 \times 10^{-4}$), and Bacteroidetes ($P_{adj} = 5.18 \times 10^{-4}$) and expansion of Proteobacteria ($P_{adj} = 1.11 \times 10^{-7}$). (*C*) On the genus level, vancomycin treatment caused a proportional decrease in *Bacteroides* ($P_{adj} = 1.07 \times 10^{-20}$), *Clostridium* ($P_{adj} = 2.31 \times 10^{-4}$), *Dorea* ($P_{adj} = 3.09 \times 10^{-9}$), *Akkermansia* ($P_{adj} = 8.00 \times 10^{-7}$), and *Parabacteroides* ($P_{adj} = 5.18 \times 10^{-5}$) compared with non–vancomycin-treated mice, and showed an increase in *Sutterella* ($P_{adj} = 1.55 \times 10^{-5}$) and *Proteus* ($P_{adj}$ 0.016) (*D*) Elimination of collagenolytic *E faecalis* and *P mirabilis* (9.4×10^6 vs 0 CFU/mg; n = 5 per group; $P < .05$, Mann-Whitney test) by using a multiple antibiotic cocktail failed to prevent tumor formation (75% vs 60%; n = 5 per group; $P = .6$, Fisher exact test) but (*E*) led to the emergence of collagenolytic *C parapsilosis*, which displayed a high capacity to degrade collagen 1 and moderate ability to degrade collagen 4. Abx, antibiotics; Surg, surgery.

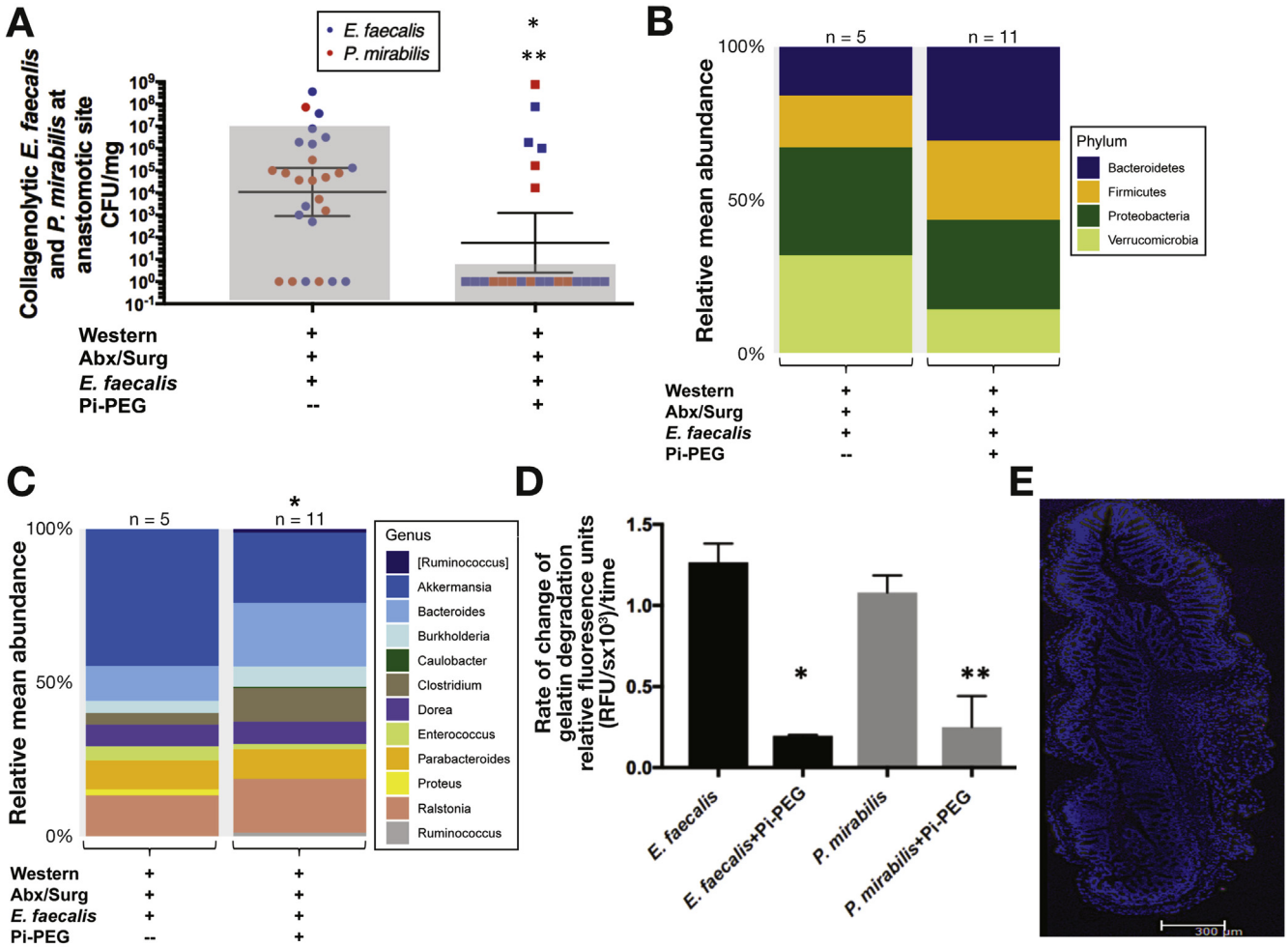

Figure 4. Pi-PEG suppresses collagenase production in vitro and decreases tumor formation in vivo. (*A*) To test the ability of the phosphate carrier compound Pi-PEG, known to attenuate bacterial collagenase in preventing tumor formation, mice were given Pi-PEG 3 days before surgery, which was continued until they were killed. Mice drinking Pi-PEG displayed a reduction by 3 orders of magnitude in collagenolytic *E faecalis* and *P mirabilis* (1.1×10^4 vs 5.6×10^1 CFU/mg; n = 15 per group; $P < .05$, Mann-Whitney) on anastomotic tissues and a 57% reduction in tumor formation (66% vs 9%; n = 15 per group; $P < .05$, Fisher exact test). (*B*, *C*) 16S ribosomal RNA gene amplicon analysis of anastomotic tissue showed no effect of Pi-PEG at the phylum level but a proportional decrease in the genus *Proteus* ($P_{adj} = 8.84 \times 10^{-4}$). (*D*) In vitro collagenase assay showing that Pi-PEG decreases the rate of collagenase production over a 20-hour incubation for both *E faecalis* (1.2×10^3 vs 0.19×10^3 RFU/time; $P < .05$, paired Student *t* test) and *P mirabilis* (1.08×10^3 vs 0.25×10^3 RFU/time; $P < .05$, paired Student *t* test). (*E*) Fluorescence in situ hybridization for *E faecalis* showed the absence of *E faecalis* in Pi-PEG–treated mouse anastomotic tissue. Abx, antibiotics; Surg, surgery.

observed in vancomycin-treated mice, and an increase in *Sutterella* ($P_{adj} = 1.55 \times 10^{-5}$), and *Proteus* ($P_{adj} = .016$) was observed (Figure 3*C*). Similarly, the absolute quantity of *Proteus* in vancomycin-treated animals was significantly increased (Supplementary Table 3).

To address the possibility that *E faecalis* and *P mirabilis* persisted in the presence of vancomycin, reiterative experiments were performed with a combination of ampicillin, spectinomycin, and streptomycin, agents specifically targeting these 2 organisms. Similarly, no difference in tumor formation was observed in non–antibiotic-treated vs penta-antibiotic–treated mice (75% vs 60%; $P = .6$, Fisher exact test). Interestingly, although bacterial cultures showed that the chosen antibiotics did eliminate tumor-associated collagenolytic *E faecalis* and *P mirabilis* (9.4×10^6 vs 0 CFU/mg; $P < .05$, Mann-Whitney test) (Figure 3*D*), we observed the emergence of *Candida parapsilosis*, a collagenolytic fungal strain. Its collagenolytic activity was confirmed by examining its ability to degrade both collagen 1 and collagen 4 (Figure 3*E*), key collagen subtypes important to maintain anastomotic integrity.

ABA-PEG20k-Pi20, a Copolymer With Known Bacterial Collagenase Suppressive Activity, Maintains Microbial Diversity and Significantly Decreases Tumor Formation

Phosphate is an environmental cue for many pathogenic bacteria, supporting their growth and suppressing virulence via highly conserved phosphosensory/

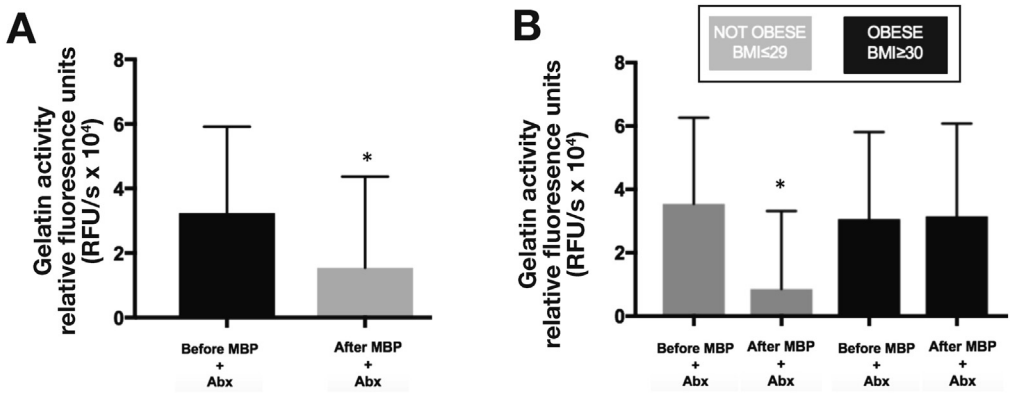

Figure 5. Effect of mechanical bowel prep and antibiotics on collagenase-producing organisms. (*A*) We surveyed patients undergoing colorectal resection for their ability to harbor collagenolytic organisms. Preoperative stool was collected before MBP, and oral antibiotics (Abx) and intraoperative stool were collected by digital rectal examination at the time of surgery. MBP reduced the quantity of collagenase-producing microbes in patients when comparing pre-MBP + Abx samples to post-MBP + Abx samples (before MBP, 3.56×10^4 vs after MBP, 2.08×10^4 RFU; before MBP, n = 48; post-MBP, n = 30, $P < .05$, unpaired Student *t* test). (*B*) MBP + Abx failed to eliminate collagenase-producing organisms in obese patients (3.2×10^4 vs 5.6×10^4 RFU; before MBP, n=14; after MBP, n = 5). MBP + Abx led to a 2-fold reduction in collagenase-producing organisms in nonobese patients (3.9×10^4 vs 1.5×10^4 RFU; before MBP, n = 34; after MBP, n = 24). Mixed-effects modeling considering repeated measurements of a subset of individuals and group-by-time interactions showed a *P* value of <.05, indicating a difference in response to MBP between normal-weight and obese patients.

phosphoregulatory elements.[32] We have previously de novo synthesized a phosphate carrier compound, Pi-PEG, and determined that it suppresses bacterial collagenase production in vitro and preserves anastomotic integrity in vivo.[10,32] Here, we tested whether a 1% solution of Pi-PEG in the drinking water given to mice throughout the study period could prevent tumor formation. Given that WD-fed mice treated with prophylactic antibiotics, surgery, and *E faecalis* administration developed the highest incidence of tumors (88% in this group), these were the conditions used for the control group. We found that mice given Pi-PEG showed a 57% reduction in tumor formation (66% vs 9%; $P < .05$, Fisher exact test) compared with controls (WD plus antibiotics) and a reduction by 3 orders of magnitude in tumor-associated collagenolytic *E faecalis* and *P mirabilis* (1.1×10^4 vs 5.6×10^1 CFU/mg; $P < .05$, Mann-Whitney test) (Figure 4*A*). Mice drinking Pi-PEG showed no significant difference in the proportion of bacterial phyla compared with controls (Figure 4*B*). However, Pi-PEG consumption resulted in a significant decrease in the proportion of *Proteus* ($P_{adj} = 8.84 \times 10^{-4}$) in Pi-PEG–treated mice compared with controls (Figure 4*C*). The absolute quantities of both *Enterococcus* and *Proteus* species were significantly decreased in the Pi-PEG cohorts (Supplementary Table 3). As a control, std-fed animals (n = 5) were treated with Pi-PEG; similar to std-fed animals without Pi-PEG, these mice did not develop perianastomotic tumors, and there was no colonization of collagenolytic organisms on the anastomotic tissue. After a 20-hour incubation period in vitro, Pi-PEG suppressed collagenase production of both *E faecalis* (1.2×10^3 vs 0.19×10^3 relative fluorescence units (RFU)/time; $P < .05$, paired Student *t* test) and *P mirabilis* (1.08×10^3 vs 0.25×10^3 RFU/time; $P < .05$, paired Student *t* test) (Figure 4*D*). Similarly, Pi-PEG reduced the ability of *C parapsilosis* to degrade both collagen 1 (15.7×10^3 vs 2.4×10^3 RFUs; $P < .05$, paired Student *t* test) and collagen 4 (5.5×10^3 vs 0.99×10^3 RFUs; $P < .05$, paired Student *t* test). Fluorescence in situ hybridization staining for *E faecalis* showed that Pi-PEG eliminated *E faecalis* in the tumor environment (Figure 4*E*). Finally, we observed no CT26 tumor cells in the liver in mice treated with Pi-PEG (n = 4).

Colonization With Collagenase-Producing Organisms Varies Among Patients Undergoing Colon Surgery

To determine the clinical relevance of our findings, we surveyed patients undergoing colorectal resection for their ability to harbor collagenolytic organisms. Preoperative stool was collected before initiation of routine mechanical bowel preparation (MBP), and oral antibiotics and intraoperative stool were collected by rectal examination at the time of surgery. As would be predicted given the antibiotics used, MBP plus antibiotics reduced the total quantity of collagenase-producing microbes in patients (before MBP, 3.56×10^4 vs after MBP, 2.08×10^4 RFU; before MBP, n = 48; after MBP, n = 29; $P < .05$, unpaired Student *t* test) (Figure 5*A*). However, when patients were stratified by body mass index, the quantity of collagenase-producing microbes in patients with obesity (BMI of >29 kg/m^2) actually increased after MBP (3.2×10^4 vs 5.6×10^4 RFU; before MBP, n = 14; after MBP, n = 5), whereas MBP decreased collagenolytic bacteria in patients with normal weight (3.9×10^4 vs 1.5×10^4 RFU; before MBP, n = 34; after MBP, n = 24). Mixed-effects modeling that considered repeated measurements of a subset of individuals and group-by-time interactions showed a *P* value of <.05, indicating a difference in response to bowel preparation between normal-weight and obese patients (Figure 5*B*).

Discussion

Technical advances and treatment options have improved outcomes for patients with CRC. However, even when a pathologically confirmed complete resection has been achieved, both local and distant metastases can occur, and the underlying mechanisms remain elusive. Data from the present study show that shed cancer cells in the colon lumen can penetrate intact anastomotic tissues, forming tumors that mimic local recurrence. We hypothesize that colonization of anastomotic tissues by collagenolytic bacteria disrupts the healing intestine, resulting in increased permeability and transmigration of cancer cells. The finding that collagenolytic bacteria are enriched in the colon of mice fed a high-fat diet is especially intriguing, given the known role of collagenolytic bacteria in the pathogenesis of anastomotic leak coupled with the knowledge that the incidence of recurrent CRC is associated with both anastomotic leak and consumption of a high-fat WD.[9,13,20] Although the precise mechanisms of shed cancer cells leading to a local recurrence or possibly distant disease after surgery is likely multifactorial and will require further study, the model described here suggests that exposure of mice to the multiple elements that encompass treatment of the human disease may be necessary.

Although understanding the role of the microbiome in the etiopathogenesis of CRC is critically important, its role in disease recurrence after surgery has received little attention. Patients routinely receive preoperative antibiotics, although the type, route, and dosing are highly variable. However, the use of a broad bacteria-killing strategy to achieve intestinal antisepsis before surgery does not consider the collateral damage inflicted on the normal microbiota and resultant increased pathogenic bacterial or fungal phenotypes that might emerge from this practice. Here, we attempted to decontaminate mice of collagenolytic bacteria before surgery with multiple antibiotics to target resistant *E faecalis* and *P mirabilis*, yet this approach was unsuccessful at reducing tumor formation. These results are consistent with enhanced tumor progression after long-term treatment with an antibiotic cocktail and depletion of the intestinal microbiome in a commonly used murine model of familial adenomatous polyposis, the $Apc^{Min/-}$ model. Theses antibiotic-treated mice had a reduction in mucus-producing goblet cells, known to be protective to the colonic epithelium and a vital nutrient source for the microbiome.[34–36] Our attempt to indiscriminately eliminate all collagenolytic pathogens resulted in the subsequent overgrowth of *C parapsilosis*, which itself is collagenolytic. The ability of this pathogen to secrete collagenase that degrades collagen 1 and 4 has not, to our knowledge, previously been described; however, it has been shown that *C parapsilosis* can emerge when patients have received multiple antibiotics.[37] The emergence of *C parapsilosis* with collagenolytic activity at the site of anastomosis suggests that, in addition to eubacteria, other members of the gut microbial community may play a yet undescribed role in rendering healing tissues vulnerable to tumor cell invasion.

Given that the standard approach to eliminate all potential pathogens resulted in severe dysbiosis and the emergence of an opportunistic pathogen, we took a more targeted approach using Pi-PEG. We have previously shown that a wide variety of microbes express enhanced virulence in a phosphate-depleted environment. Phosphate covalently linked to PEG allows it to distribute along the entire mouse intestine. Work from our laboratory has established that Pi-PEG, although it does not affect bacterial growth, increases the local phosphate concentration and, consequently, decreases microbial virulence, increases tight junctions, and promotes intestinal healing after surgery.[10,38,39] Here, we found that Pi-PEG inhibits collagenase production, *E faecalis*, *P mirabilis*, and *C parapsilosis* and protects mice from tumor formation. We also found that Pi-PEG does not disrupt the intestinal microbiome community or promote proliferation of other virulent pathogens, providing an advantage over conventional antibiotics. Although further confirmatory studies are needed, we theorize that the efficacy of Pi-PEG to reduce tumor formation in this model lies in its ability to preserve the integrity of the normal microbiota, suppress commensals from expressing a virulent collagenolytic phenotype, and decrease intestinal permeability across the healing anastomosis.

Our study has several limitations. Although the presence of collagenolytic organisms are strongly associated with tumor formation, and in their absence, no malignancy developed, we were unable to prove causality. Although technically feasible to selectively disable collagenase activity using gene editing, these studies are methodologically complex and beyond the scope of the present study. However, beyond the scope of the current study, it is possible that additional micro-organisms such as protozoa, viruses, and other fungi may play a role in tumor formation. These experiments could be repeated in germ-free mice colonized with collagenase-producing organisms and compared with strain-specific mutants lacking collagenase genes. Although this was considered, wound healing in germ-free mice is not normal, and performing colon surgery in germ-free mice can be problematic.[40] We recognized that the use of Pi-PEG alone is insufficient to establish causality between bacterial collagenase production and tumor formation, because this agent may have had other effects beyond its ability to suppress bacterial collagenase. Finally, conclusions regarding the metastatic potential beyond the confines of the perianastomotic tissues are limited because this was not the focus of the study.

Overall, our findings highlight a real need for a more complete understanding of how the combined effects of diet, antibiotic use, and surgery influence microbiome structure, membership, and function. In the context of colon cancer surgery, understanding how these factors, either permissively or actively, allow shed colon cancer cells to penetrate a surgically intact anastomosis may be important to elucidate the process of colon cancer recurrence after curative resection. The finding that MBP, including antibiotics, successfully decontaminated the colon of collagenolytic pathobiota in some but not other patients may provide a clue as to why a subset of patients develop recurrence. These

preliminary observations, if confirmed in larger-powered studies, might have significant clinical implications in the preoperative management of patients. Finally, the implications of the present study on cancer recurrence rates after curative CRC surgery suggests that longitudinal tracking of the colon microbiota with the microbiome and metabolome profiling may inform the dietary recommendations and bowel preparations needed to reduce local recurrence rates.

Supplementary Material

Note: To access the supplementary material accompanying this article, visit the online version of *Gastroenterology* at www.gastrojournal.org, and at https://doi.org/10.1053/j.gastro.2019.10.020.

References

1. Jemal A, Ward EM, Johnson CJ, et al. Annual report to the nation on the status of cancer, 1975–2014, featuring survival. J Natl Cancer Inst 2017;109(9):djx030.
2. Manfredi S, Bouvier AM, Lepage C, et al. Incidence and patterns of recurrence after resection for cure of colonic cancer in a well defined population. Br J Surg 2006; 93:1115–1122.
3. Naxerova K, Reiter JG, Brachtel E, et al. Origins of lymphatic and distant metastases in human colorectal cancer. Science 2017;357(6346):55–60.
4. Fermor B, Umpleby HC, Lever JV, et al. Proliferative and metastatic potential of exfoliated colorectal cancer cells. J Natl Cancer Inst 1986;76:347–349.
5. Umpleby HC, Fermor B, Symes MO, Williamson RC. Viability of exfoliated colorectal carcinoma cells. Br J Surg 1984;71:659–663.
6. Yu X-F, Ma Y-Y, Hu X-Q, et al. Analysis of exfoliated gastric carcinoma cells attached on surgical supplies. Onco Targets Ther 2014;7:1869–1873.
7. Gertsch P, Baer HU, Kraft R, et al. Malignant cells are collected on circular staplers. Dis Colon Rectum 1992; 35:238–241.
8. Kluger Y, Galili Y, Yossiphov J, et al. Model of implantation of tumor cells simulating recurrence in colonic anastomosis in mice. Dis Colon Rectum 1998;41:1506–1510.
9. Shogan BD, Belogortseva N, Luong PM, et al. Collagen degradation and MMP9 activation by *Enterococcus faecalis* contribute to intestinal anastomotic leak. Sci Transl Med 2015;7(286):286ra68.
10. Hyoju SK, Klabbers RE, Aaron M, et al. Oral polyphosphate suppresses bacterial collagenase production and prevents anastomotic leak due to *Serratia marcescens* and *Pseudomonas aeruginosa*. Ann Surg 2018; 267:1112–1118.
11. Shogan BD, Carlisle EM, Alverdy JC, Umanskiy K. Do we really know why colorectal anastomoses leak? J Gastrointest Surg 2013;17:1698–1707.
12. Sciuto A, Merola G, De Palma GD, et al. Predictive factors for anastomotic leakage after laparoscopic colorectal surgery. World J Gastroenterol 2018;24:2247–2260.
13. Ramphal W, Boeding JRE, Gobardhan PD, et al. Oncologic outcome and recurrence rate following anastomotic leakage after curative resection for colorectal cancer. Surg Oncol 2018;27:730–736.
14. Mirnezami A, Mirnezami R, Chandrakumaran K, et al. Increased local recurrence and reduced survival from colorectal cancer following anastomotic leak: systematic review and meta-analysis. Ann Surg 2011;253:890–899.
15. Costi R, Santi C, Bottarelli L, et al. Anastomotic recurrence of colon cancer: genetic analysis challenges the widely held theories of cancerous cells' intraluminal implantation and metachronous carcinogenesis. J Surg Oncol 2016;114:228–236.
16. Bullman S, Pedamallu CS, Sicinska E, et al. Analysis of *Fusobacterium* persistence and antibiotic response in colorectal cancer. Science 2017;358(6369):1443–1448.
17. Burns MB, Montassier E, Abrahante J, et al. Colorectal cancer mutational profiles correlate with defined microbial communities in the tumor microenvironment. PLoS Genet 2018;14(6):e1007376.
18. de Almeida CV, Taddei A, Amedei A. The controversial role of *Enterococcus faecalis* in colorectal cancer. Therap Adv Gastroenterol 2018;11:1756284818783606.
19. Turnbaugh PJ, Ridaura VK, Faith JJ, et al. The effect of diet on the human gut microbiome: a metagenomic analysis in humanized gnotobiotic mice. Sci Transl Med 2009;1(6):6ra14.
20. Meyerhardt JA, Niedzwiecki D, Hollis D, et al. Association of dietary patterns with cancer recurrence and survival in patients with stage III colon cancer. JAMA 2007; 298:754–764.
21. Mehta RS, Song M, Nishihara R, et al. Dietary patterns and risk of colorectal cancer: analysis by tumor location and molecular subtypes. Gastroenterology 2017; 152:1944–1953.
22. Zhang M, Yang X-J. Effects of a high fat diet on intestinal microbiota and gastrointestinal diseases. World J Gastroenterol 2016;22:8905–8909.
23. Martinez KB, Leone V, Chang EB. Western diets, gut dysbiosis, and metabolic diseases: are they linked? Gut Microbes 2017;8:130–142.
24. Fearnside JF, Dumas M-E, Rothwell AR, et al. Phylometabonomic patterns of adaptation to high fat diet feeding in inbred mice. PLoS One 2008;3(2):e1668.
25. Oshima G, Wightman SC, Uppal A, et al. Imaging of tumor clones with differential liver colonization. Sci Rep 2015;5:10946.
26. Guyton KL, Levine ZC, Lowry AC, et al. Identification of collagenolytic bacteria in human samples: screening methods and clinical implications for resolving and preventing anastomotic leaks and wound complications. Dis Colon Rectum 2019;62:972–979.
27. Earth Microbiome Project Website. Available at: http://www.earthmicrobiome.org/. Accessed February 6, 2020.
28. Parada AE, Needham DM, Fuhrman JA. Every base matters: assessing small subunit rRNA primers for marine microbiomes with mock communities, time series and global field samples. Environ Microbiol 2016; 18:1403–1414.
29. Bolyen E, Rideout JR, Dillon MR, et al. Reproducible, interactive, scalable and extensible microbiome data science using QIIME 2. Nat Biotechnol 2019;37:852–857.

30. Callahan BJ, McMurdie PJ, Rosen MJ, et al. DADA2: high-resolution sample inference from Illumina amplicon data. Nat Methods 2016;13:581–583.
31. Bokulich NA, Kaehler BD, Rideout JR, et al. Optimizing taxonomic classification of marker-gene amplicon sequences with QIIME 2's q2-feature-classifier plugin. Microbiome 2018;6:90.
32. Mao J, Zaborin A, Poroyko V, et al. De novo synthesis of phosphorylated triblock copolymers with pathogen virulence-suppressing properties that prevent infection-related mortality. ACS Biomater Sci Eng 2017;3:2076–2085.
33. Hyoju SK, Klabbers RE, Aaron M, et al. Oral polyphosphate suppresses bacterial collagenase production and prevents anastomotic leak due to *Serratia marcescens* and *Pseudomonas aeruginosa*. Ann Surg 2017;267:1112–1118.
34. Kaur K, Saxena A, Debnath I, et al. Antibiotic-mediated bacteriome depletion in $Apc^{Min/+}$ mice is associated with reduction in mucus-producing goblet cells and increased colorectal cancer progression. Cancer Med 2018;7:2003–2012.
35. Jakobsson HE, Rodríguez-Piñeiro AM, Schütte A, et al. The composition of the gut microbiota shapes the colon mucus barrier. EMBO Rep 2015;16:164–177.
36. Kaur K, Saxena A, Larsen B, et al. Mucus mediated protection against acute colitis in adiponectin deficient mice. J Inflamm (Lond) 2015;12:35.
37. Wong PN, Mak SK, Lo KY, et al. A retrospective study of seven cases of *Candida parapsilosis* peritonitis in CAPD patients: the therapeutic implications. Perit Dial Int 2000;20:76–79.
38. Romanowski K, Zaborin A, Valuckaite V, et al. *Candida albicans* isolates from the gut of critically ill patients respond to phosphate limitation by expressing filaments and a lethal phenotype. PLoS One 2012;7(1):e30119.
39. Long J, Zaborina O, Holbrook C, et al. Depletion of intestinal phosphate after operative injury activates the virulence of *P aeruginosa* causing lethal gut-derived sepsis. Surgery 2008;144:189–197.
40. Hooper LV, Wong MH, Thelin A, et al. Molecular analysis of commensal host-microbial relationships in the intestine. Science 2001;291(5505):881–884.

Received April 11, 2019. Accepted October 20, 2019.

Correspondence
Address correspondence to: John C. Alverdy, MD, 5841 S Maryland Ave, MC 6090, Chicago, Illinois 60637. e-mail: jalverdy@surgery.bsd.uchicago.edu; fax: (773) 834-0201.

Acknowledgments
Author contributions: Sara Gaines, Marc Bissonnette, Neil Hyman, Ralph Weichselbaum, Jack Gilbert, Eugene Chang, Olga Zaborina, Benjamin D. Shogan, and John C. Alverdy formulated the central hypothesis, conceived, and planned the experiments. Sara Gaines, Marc Bissonnette, Jack Gilbert, and Benjamin D. Shogan were directly involved in institutional review board submission and approval. Sara Gaines, Jasper B. van Praagh, Ashley J. Williamson, Richard A. Jacobson, and Sanjiv Hyoju performed murine surgical experiments. Sara Gaines, Jasper B. van Praagh, and Ashley J. Williamson performed microbial culture for collagenase. Sara Gaines, Jasper B. van Praagh, Richard A. Jacobson, and Hyun Y. Koo performed collagenase assays. Sara Gaines, Jasper B. van Praagh, and Jack Gilbert performed DNA isolation and 16s rRNA analysis. Jun Mao synthesized Pi-PEG. Lindsay Alpert reviewed necropsy specimens. Sara Gaines and Jasper B. van Praagh performed RT-PCR. Sara Gaines and Alexander Zaborin performed fluorescence in situ hybridization. Sara Gaines, Neil Hyman, Olga Zaborina, Benjamin D. Shogan, and John C. Alverdy interpreted experimental results. Sara Gaines, Benjamin D. Shogan, and John C. Alverdy were primary writers for the manuscript. All authors contributed regular feedback during the writing and editing of the manuscript.

Conflicts of interest
The authors disclose no conflicts.

Funding
This work was supported by the National Institutes of Health (NIH)/National Institute of Diabetes and Digestive and Kidney Diseases T32-DK007074-43 (Sara Gaines/Eugene Change), NIH/National Cancer Institute F32-CA228235 (Sara Gaines), University of Chicago Institute of Translational Medicine Pilot Grant (Benjamin D. Shogan), Society of Surgery for the Alimentary Tract Career Development Award (Benjamin D. Shogan), and NIH R01-GM062344-18 (John C. Alverdy).

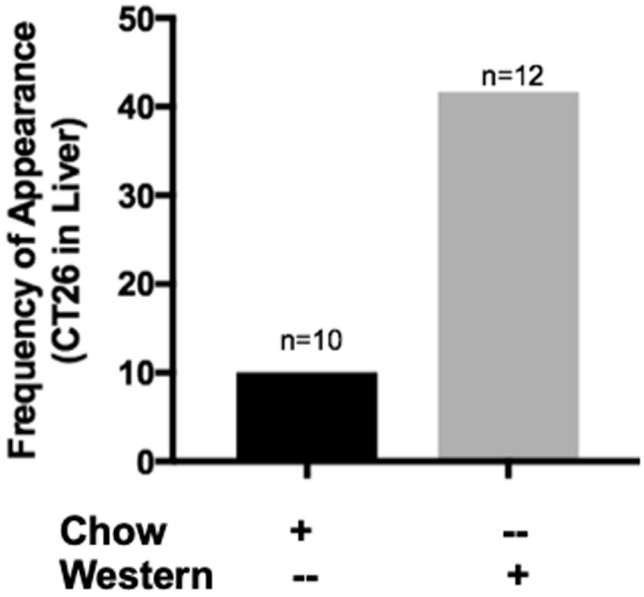

Supplementary Figure 1. WD-fed mice had a nonstatistically significant increase in liver micrometastases compared with std-fed mice (40% vs 10%; $P = .1$, Fisher exact test).

Supplementary Table 1. Nutritional Content of the Standard Murine Chow Diet Compared With the Western Diet (Bioserve S3282)

	Chow (std)	Western (WD)
Fatty acids, *g/kg*		
Total saturated	9	141
Total monounsaturated	13	162
Total polyunsaturated	34	40.2
Fat, %	6.2	36
Fiber, %		
Crude fiber	3.5	0
Neutral detergent fiber	14.7	0
Crude protein, %	18.6	20.5
Carbohydrates, %	44.2	35.7
Simple sugars	3	22
Complex sugars	41	14
Calories, *kcal/g*		
From protein	0.24	0.82
From fat	0.18	3.24
From carbohydrates	0.58	1.43
Minerals, *g/kg*		
Calcium	10	5.6
Chloride	4	0.86
Phosphorus	7	5.8
Sodium	2	0.57
Potassium	6	5.6
Magnesium	2	0.49
Zinc	0.07	0.022
Manganese	0.1	0.047
Copper	0.015	0.004
Iodine	0.006	0.003
Iron	0.2	0.05
Selenium	0.00023	0.00021
Amino acids, *g/kg*		
Aspartic acid	14	12.8
Glutamic acid	34	40.6
Alanine	11	5.3
Glycine	8	4.9
Threonine	7	8.7
Proline	16	20.5
Serine	11	11.4
Leucine	18	16.6
Isoleucine	8	11
Valine	9	13
Phenylalanine	10	8.9
Tyrosine	6	11.4
Methionine	4	7.1
Cystine	3	0.6
Lysine	9	14.8
Histidine	4	5.5
Arginine	10	7.3
Tryptophan	2	2.2
Vitamins, *mg/kg*		
Vitamin K3 (menadione)	50	0.52
Vitamin B1 (thiamin)	17	3
Vitamin B2 (riboflavin)	15	2.3
Niacin (nicotinic acid)	70	15
Vitamin B6 (pyridoxine)	18	4.1
Pantothenic acid	33	5.5
Vitamin B12 (cyanocobalamin)	0.08	0.04
Folate	4	0.75
Choline	1200	1148
Vitamins, *IU/kg*		
Vitamin A	15,000	3162
Vitamin E	110	25.7

Supplementary Table 2. Primer Sequences Used to Amplify the *Luc2* Gene in CT26 Cells

Luc2 (Taqman)	Sequence
Forward	5′-GTGGTGTGCAGCGAGAATAG-3′
Probe	5′-TTGCAGTTCTTCATGCCCGTGTTG-3′
Reverse	5′- CGCTCGTTGTAGATGTCGTTAG-3′

Supplementary Table 3. Mean Absolute Amount of the Genera *Enterococcus* and *Proteus* in Anastomotic Tissue From the Various Groups[a]

Group	*Enterococcus*, pg/μL	*Proteus*, pg/μL
Std + Abx	81	0
Std + Abx + EF	0	0
WD + Abx	465	228
WD + Abx + EF	265	627
WD +' Pi-PEG	42	2
WD + vancomycin	390	9549

Abx, antibiotics; EF, *E faecalis* enema.
[a]Calculated based on percentages of 16S ribosomal RNA gene sequencing and quantitative PCR of eubacteria primers (forward: 5′-TCCTACGGGAGGCAGCAGT-3′; reverse: 5′ GGACTACCAGGGTATCTAATCCTGTT-3′).